1999년도 한국음향학회 학술발표대회 논문집 제18권 제1(s)호

결합형 유한요소-경계요소 기법을 사용한 심해저용 압전형 유연성 쏘나 변환기의 시뮬레이션

장순석, 이제형, 안흥구, 최현호
조선대학교 공과대학 전기 · 제어계측공학부

Simulation of a piezoelectric flextentional deep-water sonar transducer using a coupled FE-BEM

Soon Suck Jarng, Je Hyeong Lee, Heung Gu Ahn, Heun Ho Choi
Dept. of Electrical Control & Instrumentation, Chosun University

Abstract

A piezoelectric flextentional deep-water sonar transducer has been simulated using a coupled FE-BEM. The dynamics of the sonar transducer is modelled in three dimensions and is analyzed with external electrical excitation conditions as well as external acoustic pressure loading conditions. Different results are available such as steady-state frequency response for RX and TX, displacement modes, directivity patterns, back-scattering patterns, resonant frequencies, bandwidths, quality factors, transmitting voltage (TV) responses, input receiving sensitivity (RS) responses. While the present barrel-stave typed sonar transducer of the piezoelectric material is being simulated, the external surface of the transducer is modified in order to allow the same water pressure to be applied to the inner and the outer surfaces of the transducer. With this modfication for deep-water application, the resonance frequency of the modified flextentional sonar transducer becomes much lower than that of the unmodified flextentional sonar transducer. The results of the present sonar transducer modelling are also compared with those of a commercial package such as ATILA.

1. Introduction

Ocean acoustic tomography requires wide bandwidth, compact, and effectively low frequency sources of sound [1]. This paper describes the modelling process for such a sonar transducer using a coupled finite element-boundary element method (FE-BEM). Flextentional sonar transducers are widely used as a high-power projector. It is a compact sound source efficiently over a broad frequency range [2]. The precise dimensions of a flextentional sonar transducer could be optimally predicted by the analysis of the flextentional transducer dynamics. The choice of the active element depends on structural types and electromechanical efficiency of the transducer. A flextentional transducer such as a barrel-stave type has been modelled in three dimensions. The main aim of this paper is to simulate the structural dynamics of the flooded piezoelectric flextentional sonar transducer using a coupled FE-BEM. Different results for analyses are produced; displacement modes, directivity patterns, back-scattering patterns, resonant frequencies, bandwidths, quality factors, transmitting voltage responses, receiving sensitivity responses.

2. Numerical Method

2.1. Coupled FE-BE Method

The following equation (1) is the integral formulation of the piezoelectric equations modelling of a sonar transducer submerged into the water [3]:

$$\begin{aligned}(F) &+ [L](A^{\oplus})^{-1}\Psi^{\oplus}_{inc} \\ &= [K_{uu}]\{a\} + [\rho_f \omega^2[L](A^{\oplus})^{-1}B^{\oplus}]\{a\} \\ &\quad - \omega^2[M]\{a\} + j\omega[R]\{a\} + [K_{u\phi}]\{\Phi\} \\ -\{Q\} &= [K_{\phi u}]\{a\} + [K_{\phi\phi}]\{\Phi\}\end{aligned} \tag{1}$$

where

$\{F\}$ Applied Mechanical Force	$\{Q\}$ External Electrical Charge
$\{a\}$ Elastic Displacement	$\{\Phi\}$ Electric Potential
$\Psi^{\oplus}_{inc}$ Incident Pressure	$[K_{uu}]$ Elastic Stiffness Matrix
$[K_{u\phi}]$ Piezoelectric Stiffness Matrix	$[K_{\phi u}]=[K_{u\phi}]^T$
$[K_{\phi\phi}]$ Permittivity Matrix	$[M]$ Mass Matrix
$[R]$ Dissipation Matrix	j $\sqrt{-1}$
$[L]$ Coupling Matrix at the Fluid-Structure Interface	
$A^{\oplus}$ Fluid BEM Matrix [A]	$B^{\oplus}$ Fluid BEM Matrix [B]
ω Angular Frequency	ρ_f Fluid Density

Incident pressure of the equation (1) is zero in case of the present sonar transmitter. The isoparametric formulation for 3 dimensional structural elements is well documented by Allik H. et. al. [4]. Each 3 dimensional finite element is composed of 20 quadratic isoparametric nodes and each node has nodal displacement (a_x, a_y, a_z) and electric potential

(ϕ) variables. Table 1 and Table 2 show property values of the materials used for the flextentional sonar transducer.

For very-low-frequency (below 2KHz) and higher-power applications flextentional transducers are generally used (Fig. 1). Here a stack of ceramic ring, as it expands and contracts as a result of the applied alternating voltage, exerts an oscillatory force on a pair of thick metal "barrel staves" [5]. A bolt holds the staves together and pre-stresses the ceramic stack so that even under high drive the ceramic and any bonds between components remain in compression. With this construction the relatively small linear motion of the ceramic stack is converted into a much larger change in the volume of the staves, so that moderate power levels are possible.

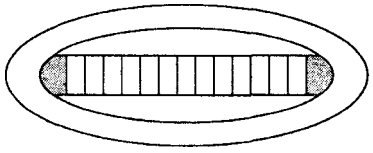

Fig. 1 Sonar transducer prototypes for frequencies below 2KHz

Table1. Piezoelectric Material Properties of PZT4 (Axially Polarized Properties)

Para-meter	Value	Unit	Para-meter	Value	Unit
ρ	7500	Kg/m^3	C_{xy}^{x}	3.06E+10	N/m^2
C_x^x	1.39E+11	N/m^2	$e_{p,z}^{x}$	-5.2	N/Vm
C_y^x	7.78E+10	N/m^2	$e_{p,z}^{y}$	-5.2	N/Vm
C_z^x	7.43E+10	N/m^2	$e_{p,z}^{z}$	15.1	N/Vm
C_y^y	1.39E+11	N/m^2	$e_{p,z}^{yz}$	12.7	N/Vm
C_z^y	7.43E+10	N/m^2	$e_{p,z}^{zx}$	12.7	N/Vm
C_z^z	1.15E+11	N/m^2	ϵ_x^x	6.46E-9	F/m
C_{yz}^{yz}	2.56E+10	N/m^2	ϵ_y^y	6.46E-9	F/m
C_{zx}^{zx}	2.56E+10	N/m^2	ϵ_z^z	5.62E-9	F/m
K_{33}	0.69	-	K_{15}	0.70	-

Table 2. Properties of other materials used for the FFR sonar transducer

Property / Material	Density ρ [Kg/m^3]	Young's Modulus Y [N/m^2]	Poison's Ratio γ
Air	1.22	1.411E5	-
Aluminium	2750	70.0E9	0.34
Steel	7850	207.0E9	029

2.2. Modelling of a barrel-stave typed piezoelectric sonar transducer

Instead of using the piezoelectric ceramic itself in a flexural mode, it is possible to devise flextentional structures in which the high stress but low strain generation of the ceramic in the thickness mode is transformed into larger displacements by means of some type of level action (Fig. 1~Fig. 3). A stack of piezoelectric ceramic operating in the thickness mode is connected to a surrounding elliptical shell like a barrel-stave. When the stack extends, along the major axis of the ellipse, the shell moves inwards along the minor axis, thus producing a large volume displacement overall. In general terms, the resonance frequency of such a transducer depends principally on the major and minor axes, wall thickness, and material properties of the shell, with the stack itself having a lesser influence [6]. The bandwidth is also dependent primarily on the parameters of the shell. Maximum eccentricity leads to the maximum bandwidth, but has the lowest power output, whist least bandwidth and highest power occurs for the least eccentric shape [6]. The maximum pressure which an elliptical shell can withstand is also dependent on its shape and thickness, and is therefore related to its resonance frequency. The size of the flextentional transducer is generally much less than a wavelength in water at their resonance frequency. It therefore radiates approximately omni-directionally in the plane perpendicular to the major axis. A compressive pre-stress needs to be applied to the stack for higher power output from a compact size. This is usually done by applying pressure to the minor axis of the shell, thus extending the major axis, and inserting the stack into the extended shell. On release of the pressure, the relaxation of the shell applies the necessary force to the stack.

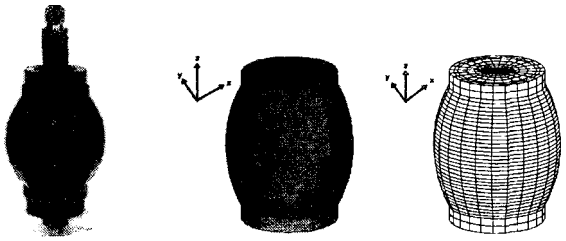

(a) (b) (c)

Fig. 2 External view of the flextentional sonar transducer (a) and their corresponding finite mesh elements in 3 dimensions (b) and (c).

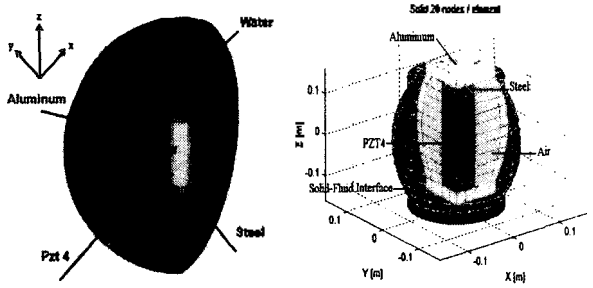

(a) (b)

Fig.3 Three dimensional view of the flextentional sonar transducer within the fluid domain (a) and the internal materialistic composure of the modelled sonar transducer (b).

The piezoelectric flextentional sonar transducer has been totally divided into 608 elements with 3280 nodes. The solid-fluid interfacing surface elements are 320 with 992 nodes. Only one fourth of the total

elements are used for formulation of the global coefficient matrix because of the symmetricity of the structure as shown in Fig. 3 (b). The resulted size of the global coefficient matrix is 3876 by 3876. One important point for loading of electric charges on piezoelectric ceramics is that the typical ratio between the charges on the vertex node and on the midside node is -1:4 for the present parabolic shape function of the Serendipity family [4]. The principle of the superposition is applied to common nodes on adjacent elements. Fig. 4 shows the dimensions of the one eighth of the barrel-stave transducer in meter scale. The dimensions of the modelled transducer are not optimal, however the dimensions could be changed for any particular optimal purpose.

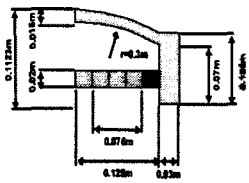

Fig. 4
The dimensions of the 1/8 of the flextentional sonar transducer.
r=curvature radius.

2.3. ATILA FE Code

ATILA is an user interactive finite element code originally developed by many French scientists and engineers during 1980s and is particularly useful for modeling piezoelectric and magnetostrictive transducers radiating into the fluid [7]. To model a radiating elastic or piezoelectric structure using ATILA, the finite element mesh must contain the structure as well as part of the fluid domain. The following equation (2) is the integral formulation of the piezoelectric equations modelling of a sonar transmitter according to ATILA:

$$\begin{aligned} \underline{F} &= \{[K_{uu}] - \omega^2[M] \\ &\quad - [L][\frac{[H]}{\rho^2 c^2 \omega^2} - \frac{[M_1]}{\rho^2 c^2} - \frac{[G]}{\rho^2 c^2 \omega^2}]^{-1}[L]^T \\ &\quad + j\omega[R]\}\underline{U} + [K_{u\phi}]\underline{\Phi} \\ \frac{-I}{j\omega} &= [K_{\phi u}]\underline{U} + [K_{\phi\phi}]\underline{\Phi} \end{aligned} \quad (2)$$

where

$\underline{F}$	Applied Mechanical Force	I	External Electrical Current
$\underline{U}$	Elastic Displacement	$\underline{\Phi}$	Electric Potential
$\underline{P}$,	Incident Pressure	$[K_{uu}]$	Elastic Stiffness Matrix
$[K_{u\phi}]$	Piezoelectric Stiffness Matrix	$[K_{\phi u}]=[K_{u\phi}]^T$	
$[K_{\phi\phi}]$	Permittivity Matrix	$[M]$	Mass Matrix
$[R]$	Dissipation Matrix	c	Fluid Sound Speed
$[L]$	Coupling Matrix at the Fluid-Structure Interface		
$[H]$	Fluid Stiffness Matrix	$[M_1]$	Fluid Mass Matrix
$[G]$	Frequency-Dependent Complex Linear Operator		
ω	Angular Frequency	ρ	Fluid Density

An appropriate radiation condition is applied to the external fluid surface boundary which surrounds the fluid domain. The $\underline{\Psi}$ vector defines the radiation condition on the external surface S limiting the fluid domain:

$$\underline{\Psi} = -\frac{\frac{1}{R}+\frac{j\omega}{c}}{\rho c}[D]\,\underline{P} + \frac{\frac{1}{R}-\frac{j\omega}{c}}{\rho c(1+\frac{\omega^2 R^2}{c^2})}[D']\,\underline{P} \quad (3)$$
$$\equiv \frac{[G]}{\rho c^2}\underline{P}$$

where R is the radius of the boundary surface S. $[D]$ and $[D']$ are obtained by assembling the damping elements on that surface. The first term is the monopolar contribution associated with a spherical wave impedance condition and the second term is the dipolar contribution [8,9]. Others use infinite fluid elements representing zero fluid pressure at S as radiation conditions [10,11]. Such methods for solving radiation condition in the far field are attempted mainly because the finally assembled global matrix equation can become symmetric. More complete solution is possible by using boundary element method (BEM) where the global matrix equation becomes non-symmetric [12,13]. Once elastic displacements on the fluid-structural interface $\underline{U}$ is known, the acoustic pressure in the far field $\underline{P}$ is calculated as

$$\underline{P} = \rho^2 c^2 \omega^2 \,[[H] - \omega^2[M_1] - [G]]^{-1}\,[L]^T\,\underline{U} \quad (4)$$

The piezoelectric flextentional sonar transducer including the fluid has been divided into 2136 elements with 4514 nodes for the two dimensional ATILA solution (Fig. 5). The structural and the fluid elements are 68 and 1928 respectively. And 52 elements are interfacing elements between the solid structure and the fluid. Also 88 elements are damping elements representing radiation conditioning elements.

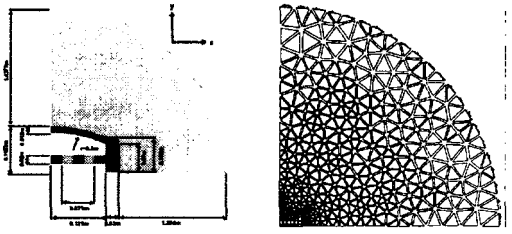

(a) (b)

Fig.5 The dimensions of the flextentional sonar transducer (a) and their structural and fluid elements for ATILA (b).

3. Results and Discussions

The coupled FE-BE method has been programmed with Fortran language running at a SUN workstation. Calculation is done with double precision and the program is made for three dimensional structures. It is a common practice to have the size of the largest element to be less than $\lambda/3$. In this paper the interest frequency of the acoustic radiation is less than 2KHz, so that $\lambda/3$ is about 0.25m. Fig.

6 shows the displacement modes of the one fourth of the total structure at 767Hz which is the resonance frequency of the present sonar transmitter. The figures are plotted with hidden lines in series for 1/20 intervals of one cycle, so that the change of the structural displacement can be viewed in different phases. From the series of figures in different phases, it is clear to notice that the force generated by the active element is transferred to the aluminium stave through the end caps in the similar mechanism like an arm lever. Therefore the relatively small linear motion of the ceramic stack is converted into a much larger change in the volume of the staves.

Fig. 7 shows the beam patterns of the transducer at 767Hz in polar form (a) and in rectangular form (b). And Fig. 8 shows the same beam pattern in three dimension. Fig. 9 shows the transmitting voltage (TV) responses of the PZT4 flextentional submerged transducer. The upper and the lower dotted lines are for the TV responses at 90° direction (X-Y plane) and at 0° direction (Z-axis) calculated by the ATILA. And the upper (+) and the lower (o) symboled lines are for the TV responses at 90° direction and at 0° direction calculated by the present coupled FE-BEM. Both results are almost perfectly agreed each other. The resonance frequency of the present flextentional transducer model is 767 Hz. And the acoustic power at the resonance is about 66.18 dB (ref 1 μPa at 1m) at 0° direction. The 3dB bandwidth and the quality factor are 435 Hz and 1.76 respectively. Fig. 10 shows acoustic radiation impedance (Ri + j Xi) as a function of frequency. And fig. 11 shows beam patterns for different input frequencies.

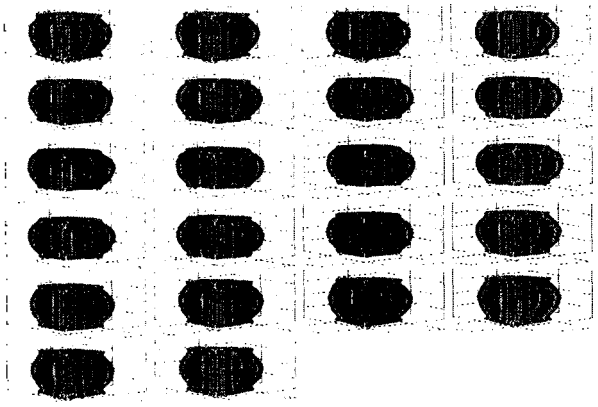

Fig. 6 Displacement modes of the one fourth piezoelectric flextentional transducer at 767Hz with different phases

Fig. 12 shows the transmitting voltage response (Fig. 10(a)) and the receiving sensitivity response (Fig. 10(b)) of the PZT4 flextentional flooded transducer calculated. by the coupled FE-BEM. The receiving sensitivity response is calculated with different frequencies by applying external pressure incident on the transducer instead of external electric charge. The pressure loading is directed either in the Z-axis or in the X-axis. Then by the piezoelectric mechanism the transducer can produce potential differences between the two electrodes. The applying pressure is kept constant to be as 1 [Pascal] throughout all input frequencies. The resulted receiving sensitivity response comparatively shows very similar patterns as the transmitting voltage responses with regard to directivity.

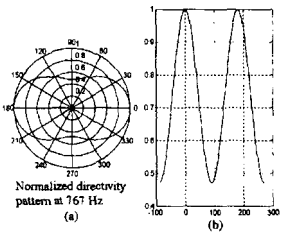

Fig. 7 Beam patterns of the flextentional piezoelectric sonar transducer at 767 Hz in polar form (a) and in rectangular form (b).

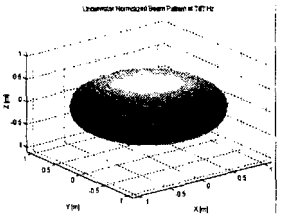

Fig. 8 Beam patterns of the flextentional piezoelectric sonar transducer at 767 Hz in three dimension.

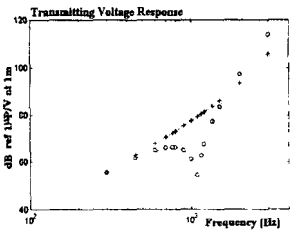

Fig. 9 Transmitting voltage response of PZT4 flextentional submerged transducer.(Solution by ATILA: Upper Dotted Line:90° Direction, Lower Dotted Line:0° Direction) (Solution by Coupled FE-BEM: Upper+Symboled Line:90° Direction, Lower o Symboled Line: 0° Direction) dB (ref 1 μPa at 1m)

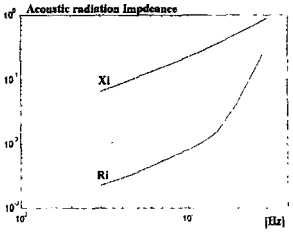

Fig. 10 Acoustic radiation impedance (Ri + j Xi) as a function of frequency.

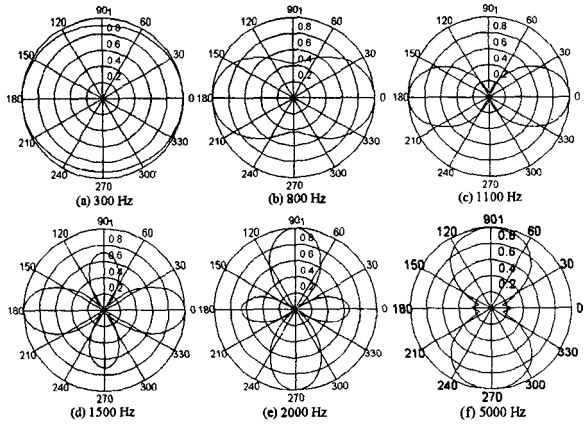

Fig. 11. Beam patterns for different input frequencies.

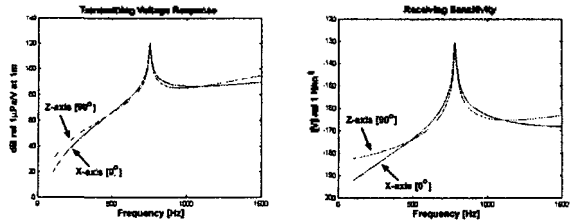

(a) (b)

Fig. 12 Transmitting voltage response (a) and receiving sensitivity response (b) of PZT4 flextentional flooded transducer calculated by the coupled FE-BEM

Fig. 13 and Fig. 14 show radial expressions of back-scattered pressures with the Z-axial (Fig. 13) and the X-axial (Fig. 14) incident pressure loadings respectively.

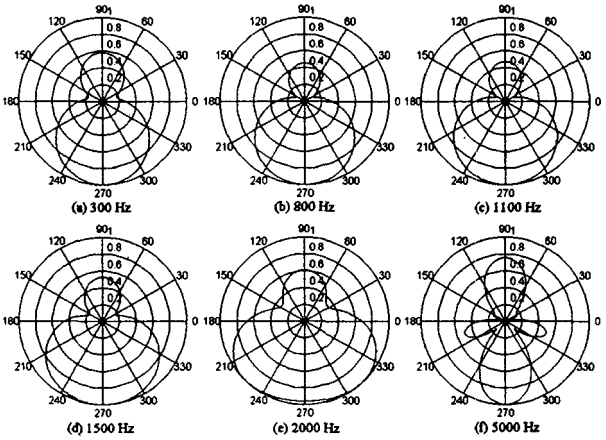

Fig. 13 Radial expressions of back-scattered pressures with the Z-axial incident pressure loading.

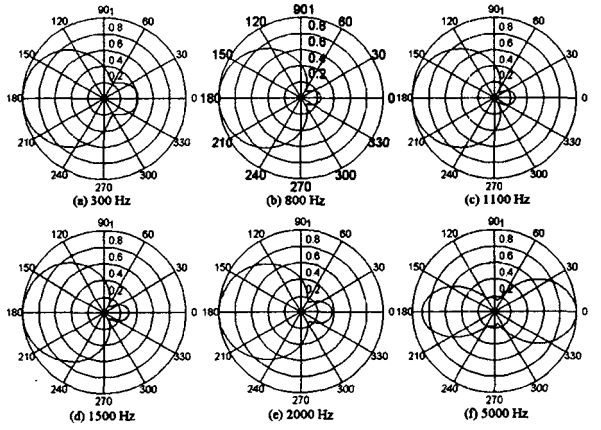

Fig. 14 Radial expressions of back-scattered pressures with the X-axial incident pressure loading.

Fig. 15 shows the displacement modes with Z-axis incident pressure loading of the one fourth piezoelectric flextentional transducer at 800Hz with different phases

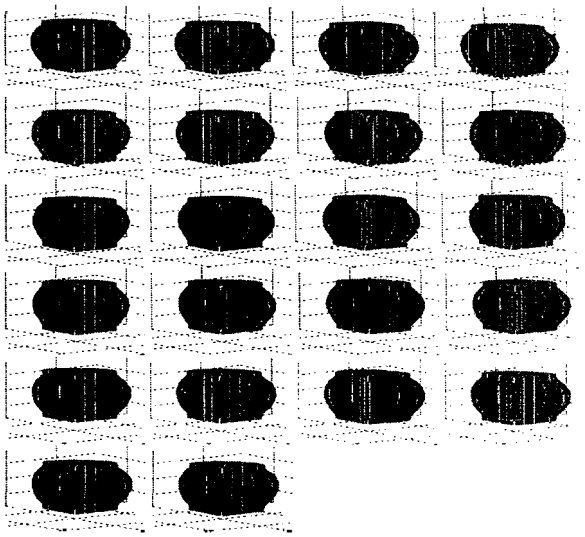

Fig. 15 Displacement modes with Z-axis incident pressure loading of the one fourth piezoelectric flextentional transducer at 800Hz with different phases

So far, the inside of the present flextentional sonar transducer is only filled with air. If the air-filled flextentional sonar transducer is submerged into deep water, the external surface of the barrel-stave is pushed into the inside by high water pressure. This deep-water pressure problem causes weakening of the structutral displacements, so that the output acoustic power becomes low. This problem can be solved by allowing the sea water to be penetrated into the inside of the transducer by some slight modification of the external surface of the barrel-staves typed flextentional transducer as shown in Fig. 16. Very narrow and long openings are made between staves, so that the inner and the outer surfaces of the stave have equal water pressure. Since the piezoelectric elements are directly exposed to water pressure loading, the resonance frequency of the modified flextentional sonar transducer becomes lower than that of the non-modified flextentional sonar transducer becasue of mass loading effects. Fig. 17 and Fig. 18 show the TVR and the directivity pattern of the modified flextentional sonar transducer. The beam pattern becomes almost omnidirectional at the resonance frequency.

4. Conclusion

The dynamics of the barrel-stave sonar transducer of the piezoelectric material had been simulated using a coupled FE-BEM. The flextentional displacement mode was temporally figured to show the mode in different phases. This paper does not include the effect of hydrostatic pressure which is significantly important for deep water operation. More advanced structural design should be considered for deep-water application such as a free-flooded flextentional transducer [14]. In conclusion, this

presented coupled FE-BEM code can be used for the design and the analysis of sonar transducers in many different aspects in material and in structure. Last 20 years have been spent for the development of other software design tools like ATILA [9,15], ANSYS [16] and PHOEBE [17], PAFEC for sonar transducer design. ATILA and ANSYS use only finite elements instead of boundary elements for radiation conditions in the fluid. PHOEBE and PAFEC use boundary elements for the radiation condition but its calculation is done in single precision. The present coupled FE-BEM uses both boundary elements for radiation conditions in the fluid and double precisions for more correct computational results.

ACKNOWLEDGEMENTS

This study was supported by a grant from STEPI (Science and Technology Policy Institute) Korea under contract I-03-020, as part of the 1998 international programme of collaboration between Korea and the United Kingdom and by a grant from the European Community under contract MAS3-CT95-0031 (BASS).

References

[1] D.T.I.Francis, J.Ahmad, C,Bayliss and R.F.W.Coates, "Finite and bounadry element modelling of class III flextentional transducers for ocean acoustic tomography", Proc. Second European Conf. Underwater Acoustics, Vol. 1., pp:515-520, 1994.

[2] D.T.I.Francis, C.Bayliss, J.Ahmad and R.F.W.Coates, "The development of a low frequency barrel-stave transducer for tomographic application using finite element and boundary element modelling", IEEE Proc. Oceans 94, Vol. 1, pp:371-376, 1994.

[3] S.S.Jarng, "PZT5 spherical hydrophone simulation using a coupled FE-BE method", J. of the Korean Sensors Society, Vol. 7, No. 6, pp:377-385, 1988.

[4] H. Allik and T.J.R. Hughes, "Finite element method for piezoelectric vibration", Int. J. Numer. Method Eng., Vol. 2, PP:151-157, 1970.

[5] Smith B.V., "Lecture notes on basic electromechanical transducer equivalent circuits for underwater applications", Edited by B. Gazey, P. McQueen and B. Smith, Post-Experience Cource on Underwater Acoustics and Sonar Systems, Vol. 1, Chapter 6, 1989.

[6] D.Stansfield, "Underwater electroacoustic transducers", Bath University Press and Institute of Acoustics, pp:354-361, 1991.

[7] ATILA Finite-Element Code for Piezoelectric and Magnetostrictive Transducer Modeling Vesion 5.03 User's Manual, Edited by Acoustics Laboratory, Institut Sup'erieur d'Electronique du Nord, Published by MAGSOFT Co., Sep. 1993.

[8] R. Bossut and J.N. Decarpigny, "Finite element modeling of radiating structures using dipolar damping elements", J. Acoust. Soc. Am. Vol. 86, No. 4, PP:1234-1244, 1989.

[9] B. Hamonic, J.C. Debus and J.N. Decarpigny, "Analysis of a radiating thin-shell sonar Transducer using the finite element method", J. Acoust. Soc. Am. Vol. 86, No. 4, PP:1245-1253, 1989.

[10] J.M.M.C. Marques and D.R.J. Owen, "Infinite elements in quasi-static materially nonlinear problems", Comp. & Struc., Vol. 18(4), PP:739-751, 1984.

[11] J.P.E. Goransson and C.F. Davidsson, "A three dimensional infinite element for wave propagation", J. Sound & Vibration, Vol. 115(3), PP:558-559, 1987.

[12] H.A. Schenck, "Improved integral formulation for acoustic radiation problems", J. Acoust. Soc. Am. Vol. 44, PP:41-58, 1968.

[13] A.J. Burton and G.F. Miller, "The application of integral integration methods to the numerical solutions of some exterior boundary problems", Proc. R. Soc. London, Ser. A 323, PP:201-210, 1971.

[14] J.Ahmad, D.T.I.Francis and R.F.W.Coates, "A fluid-filled flextentional device for ocean acoustic tomography", IEEE Proc. Oceans 95, Vol. 3, pp: 2021-2026, 1995.

[15] Hamonic B., "Application of the finite element method to the design of power piezoelectric sonar transducers", Proceedings of the International Workshop on Power Sonic and Ultrasonics Transducers Design, Edited by Hamonic B.F., Decarpigny J.N., Published by Springer-Verlag, PP:143-159. 1988.

[16] Ostergaard D.F., "A coupled field finite element for magnetostructural analysis", J. Appl. Phys., Vol. 63, No. 8, PP:3185-3187, 1988.

[17] A.Di Meglio, D.T.I.Francis and R.F.W.Coates, "PHOEBE: a 3D transducer modelling environment", Proc. Third European Conf. Underwater Acoustics, Vol. 1, 1996.